2020

Rab39 and Klp98A are Required for Furrow Formation During Early Drosophila Embryogenesis

Megan R. Millage
University of Denver

Rab39 and Klp98A are Required for Furrow Formation During Early *Drosophila* Embryogenesis

---

A Thesis

Presented to

the Faculty of the College of Natural Sciences and Mathematics

University of Denver

In Partial Fulfillment

of the Requirements for the Degree

Master of Science

---

by

Megan R. Millage

August 2020

Advisor: Todd Blankenship

Author: Megan R. Millage
Title: Rab39 and Klp98A are Required for Furrow Formation During Early *Drosophila* Embryogenesis
Advisor: Todd Blankenship
Degree Date: August 2020

ABSTRACT

The formation of a plasma membrane furrow is an essential process during development. Furrow formation is necessary for successful cell division and cytokinesis in addition to the ability to create multicellular tissues. Here, I will explore the role of the Golgi-associated Rab protein Rab39 in furrow formation during early *Drosophila* embryogenesis. Rab39 is one of eight Rab proteins that has been shown to localize to discrete puncta by live imaging in early *Drosophila* embryos, but its function and pathway have not been well characterized. In this thesis will I show that Rab39 forms dynamic, tubular structures that colocalize with trans-Golgi markers and the knockdown of Rab39 using RNA interference causes defects in furrow length and nuclear division during syncytial cycles 10-13. Klp98A, a kinesin 3 family motor protein, produces similar abnormalities when disrupted and colocalizes with Rab39. In the absence of Rab39, Klp98A strongly relocalizes to large nuclear fragments outside of the nuclear envelope that have arisen from the defects in furrow formation. Additionally, Rab39 and Klp98A dynamics are dependent on microtubule networks. Together, these proteins could represent a novel pathway that mediate membrane trafficking from the Golgi to the plasma membrane to aid in furrow formation.

TABLE OF CONTENTS

LIST OF FIGURES

INTRODUCTION

Early *Drosophila* embryogenesis

As with most sexually reproducing organisms, the first diploid nucleus in *Drosophila melanogaster* is formed after fertilization. The resulting embryo undergoes 9 rounds of syncytial division that occur deep within the yolk, however, during the 10^{th} cycle of this division the nuclei begin to migrate to the periphery of the embryo. Microtubule networks surrounding these nuclei mediate the migration from the yolk by repelling adjacent nuclei causing outward movement (Baker et al. 1993). This cortical migration leads to a monolayer of nuclei that will subsequently become a complete epithelial sheet. The formation of this epithelial sheet involves the formation of membrane furrows on the prospective apical surface of the cells that ingress and recede throughout syncytial cycles 10-13 until cycle 14 in which the nuclei become fully encapsulated by a membrane in a process called cellularization. Cellularization thus creates an epithelial sheet, which can then give rise to the three primary germ layers via gastrulation and posterior midget invagination. These processes give rise to the mesoderm and endoderm tissues, respectively.

Syncytial Furrow Formation

Once nuclei have migrated to the periphery of the embryo, they rely on transient membrane furrow formation to maintain adequate density and cortical arrangement. The first furrows form during cycle 10, and only reach approximately 1.5 μm before receding. With each cycle the furrows progressively become longer, with furrows just over 2 μm deep forming during cycle 11, 5 μm during cycle 12, and 8 μm during cycle 13. The furrows also undergo other morphogenetic changes. As they become longer with each progressive cycle, they also become more regular and organized in shape. The dynamics of these cycles change over time, as cycle 10 and 11 are driven by a single ingression phase (Ingression I) where the furrows reach their maximal cycle length before stabilizing and then eventually receding. Cycles 12 and 13 continue to increase furrow size after the stabilization phase via a second ingression phase (Ingression II), which results in the 4-fold increase in furrow length. This stage of embryonic development is when the midblastula trasition (MBT) takes place, and the zygotic genome becomes transcriptionally active. During furrow formation, Ingression I relies on maternal gene products, whereas Ingression II is dependent on the transcription of the zygotic genome. Disruption of zygotic transcription either with drugs or with mutations results in the disappearance of Ingression II and thus significantly shorter furrows (Xie and Blankenship 2018). The obligatory nature of this process is exemplified in that defects in the ability to form proper furrows leads to failures in mitosis and genomic instability. For

example, when membrane addition is disrupted in RalA mutants, the resulting shallow furrows cause polyploid nuclei to form either from mitotic collapse or fusion of adjacent nuclei (Holly et al. 2015).

Rab GTPases

Rab GTPases have been widely considered as the "master regulators" in membrane trafficking. They are often used as markers of different membrane bound compartments due to their distinct localization. For example, some of the most well studied Rabs include Rab5 on early endosomes, Rab7 on late endosomes, and Rab6 on the Golgi. They are able to mediate the trafficking of vesicles by interacting with different effectors, which are often motor or tethering proteins (Pfeffer 2005). Together, they ensure the precise transportation, docking, and fusion of these vesicles. In order to interact with their associated effectors they must be converted from their inactive GDP-bound state into their active GTP-bound state, which is accomplished by guanine nucleotide exchange factors (GEFs). GTPase activating proteins (GAPs) mediate the opposite process, where GTP is hydrolyzed into GDP. Rabs also undergo another form of regulation that is partially coupled to the nucleotide cycle, where they undergo a membrane insertion and extraction cycle. GDP dissociation inhibitor (GDI) binds to prenylated Rabs in the GDP-bound state and keep them in the cytosol by masking their isoprenyl anchor. The Rab can only be inserted into the membrane when the integral

membrane protein GDF displaces GDI (Grosshans et al. 2006). Over 60 different Rabs have been identified in mammalian cells, and because of this diversity they can be differentially expressed across tissues and partake in specialized transport pathways. (Grosshans et a. 2006) Not surprisingly, Rabs have been implicated in multiple developmental disorders, some including Hereditary Sensory and Autonomic Neuropathy, Carpenter Syndrome, and Griscelli Syndrome. They have also been associated with the progression of multiple types of cancers. (Mitra et al. 2010; Recchi and Seabra 2012; Zhang et al. 2007). Thirty-one Rab proteins have been identified in *Drosophila*, which is reflective of the decrease in complexity of trafficking pathways compared to vertebrates. Studying Rab protein function in *Drosophila* can be useful because the decreased number of expressed Rabs reduces the likelihood of redundant gene functions, most developmental signaling pathways are evolutionarily conserved from *Drosophila* to humans, and *Drosophila* genetics can be easily manipulated for study (Zhang et al. 2007).

Rab39 distribution and function

Rab39 is one of the less studied Rab proteins, despite being widely distributed in various human tissues and cell lines. Although it has been shown to localize to the Golgi, not much is known about its role in membrane trafficking. In human cells, there are two isoforms of Rab39, Rab39a and Rab39b. There is evidence that Rab39a is involved in the

late endocytic pathway, whereas Rab39b has been implicated in the early secretory pathway (D'Souza et al. 2019; Chen et al. 2003). The movement of Rab39 vesicles has been shown to be microtubule dependent, as nocodazole (microtubule disrupting agent) impairs vesicle motility (D'Souza et al. 2019).

Motor Proteins

One way Rabs mediate the accurate trafficking of vesicles is by interacting with motor proteins, which are either actin or microtubule dependent. These motor proteins drive the movement of vesicles via ATP hydrolysis, using the cytoskeletal elements as scaffolding. Microtubule dependent motors can be broken down into Kinesins and Dyneins (Grosshans et al. 2006). Most Kinesin motor proteins move vesicles towards the plus ends of microtubules which bring them towards the cell cortex, while Dyneins travel towards the minus end of microtubules to the center of the cell. An example of an interaction between a Rab GTPase and a microtubule based motor protein is Rab6A and Rabkinesin-6. Rab6 and Rabkinesin-6 localize to the trans-Golgi and have been shown to be important for successful cytokinesis in Hela cells (Echard et al. 1998)(Hill et al. 2000).

Klp98A in vesicle transport

Kinesin 3 family member kinesin-like protein at 98A (Klp98A) is a possible candidate for an effector of Rab39, as another motor protein from the same family, unc-

104, has been shown to have interactions with Rab39 (Gillingham et. al. 2014). There are still few studies on the function of Klp98A, however, the ones that have been published put Drosophila Klp98A or it's mammalian homologue KIF16B somewhere in the endo-lysosomal pathway (Derivery et al. 2015; Li et al. 2020; Mauvezin et al. 2015). Klp98A has been shown to be involved with the proper distribution of late endosomes, lysosomes, and autolysosomes and a possible upstream effector of Rab14 in *Drosophila* S2 cells (Mauvezin et al. 2015). It has also been implicated in the asymmetric segregation of signaling endosomes during sensory organ precursor division during *Drosophila* development (Derivery et al. 2015).

Thesis Specific Aims

The purpose of this thesis is to understand the role of Rab39 in directing membrane traffic during syncytial furrow formation, and to begin to piece together its pathway and effectors. I employ live-imaging and immunostaining techniques to visualize Golgi, Rab39, and Klp98A compartment dynamics and localization in syncytial embryos. Membrane furrow lengths and dynamics are measured in control embryos and embryos with shRNA knockdown of either Rab39 or Klp98A to determine their role in furrow formation. Golgi dynamics are also studied in these knockdown conditions. The relationship between Rab39 and Klp98A is explored by looking at their colocalization and by studying the effects of Rab39 knockdown on Klp98A distribution. These data

provide insight on the function and mechanism of Rab39 in Golgi-mediated membrane addition during syncytial furrow formation in early *Drosophila* development.

MATERIALS & METHODS

Fly stock and genetics

All fly stocks were maintained and collected at 25^{o} C, except for Valium and Walium lines, which were collected at 18 ^{o} C. All UAS transgenic flies were crossed with matαTub-Gal4VP16 67C;15 maternal driver females (D. St Johnston, Gurdon Institute, Cambridge, UK), and second-generation embryos were analyzed. The following fly stocks were used in this study: Oregon R BL-5, His2Av:RFP BL-23650 and BL-23651 (chromosomal marker), Resille:GFP (plasma membrane and furrow marker), Spider:GFP (plasma membrane and furrow marker), endogenous Rab39:YFP BL- 62560, Rab39 Valium22 BL-51689, UASp-Rab39:YFP BL-9825, Klp98A Valium20 BL-39037, UAS-GALT:RFP BL-65251 (Golgi marker) were obtained from the Bloomington *Drosophila* Stock Center. UASp-Rab39:mcherry (Blankenship Lab), Rab39 Walium 20 (Blankenship Lab), Klp98 Walium22 (Blankenship Lab).

Fluorescence Microscopy

Live imaging of embryos was performed on a spinning-disk confocal microscope from Zeiss/Solamere Technologies Group with 63X/1.4NA objective lens. In order to prepare them for imaging, embryos were collected from apple juice agarose plates before being

dechorionated with 50% bleach solution. Embryos were then relocated to a slide with a gas-permeable membrane in Halocarbon 27 oil (Sigma), covered with a coverslip, and imaged. For slow movies, images were acquired in 30s intervals with 27-30 z slices at a 0.5 μm interval. Fast movies involved a single z slice and 0.5-1s intervals. Fixed specimen were imaged with an Olympus Fluoview FV1000 confocal laser scanning microscope with a 60×/1.42NA objective.

Embryo Fixation and Immunostaining

Embryos were prepped for immunostaining by being dechorionated in 50% bleach solution and fixed for 1hr to 1hr 15min at the interface of heptane and 3.7% formaldehyde in 0.1 M sodium phosphate buffer (pH 7.4). They were then manually devitellinized and stained with mouse anti-GFP (1:100; Molecular Probes, A11120), mouse anti-Lamin (1:100; DSHB), or rabbit anti-Klp98A (1:100; Derivery 2015). Secondary antibodies conjugated with Alexa 488 or Alexa 568 (Molecular Probes) were used a 1:500 dilution. Embryos were mounted in Prolong Gold with DAPI (Life Technologies) to stain the nuclei for staging purposes.

Time-lapse and fixed image editing and quantification

Spinning-disk and laser-scanning images were edited with ImageJ or Photoshop, and images were leveled identically between samples.

Membrane Furrow Measurements

Embryos containing membrane (Resille:GFP or Spider:GFP) and histone markers (his2A:RFP) were live imaged. The point where apical membranes begin to meet and have a common width was determined to be the most apical z-layer. Progressive furrow ingression was measured by tracking the most basal point of a 4-5 "cell" region over time. The morphology of the marked DNA was used to determine both stage and cell cycle status, where interphase was marked by the formation of new nuclei until the chromatin began to condense, prophase was defined as the period between chromosomal condensation and nuclear membrane disassembly, metaphase started after nuclear disassembly and ended at the beginnings of chromosomal segregation, and anaphase/telophase was the period between chromosomal segregation to the formation of new daughter nuclei (Xie and Blankenship, 2018).

Nuclear fallout measurements

The amount of nuclear fallout in shRNA embryos was determined by counting the total amount of nuclei (marked with Histone:RFP) in the collected frame during one cycle and calculating the predicted amount for the next cycle by multiplying that value by two. The actual amount was measured for that cycle and then the percentage of remaining nuclei was calculated by dividing the actual value by the expected value.

Colocalization

Colocalization between Rab39 and Klp98A was performed on fixed images. Rab39 puncta ≥ 4 pixels in area (Solamere spinning disk; pixel size = 0.164 μm/pixel) were selected. The selected puncta were then overlaid with the opposing Klp98A channel. When the overlapping region was equal or larger than 2 × 2 pixels, the relationship between two proteins was determined as "colocalized." Percent colocalization was calculated by dividing the number of colocalized puncta by the total number of puncta. This was repeated over 3 z layers to determine if the distribution changed along the apico-basal axis.

Compartment Size, Intensity, and Velocity Measurements

Golgi and Rab39 velocity measurements were performed on time-lapse images. Rab39 or Golgi puncta equal to or larger than 1 pixel (Solamere spinning disk; pixel size = 0.164 μm/pixel) were selected. The movement of the selected puncta were then tracked over time. Absolute velocity was defined by the distance between the initial position and the final position of a group of selected puncta after one minute. When a given puncta moves more than 5 pixels in 10 seconds, the movement was determined as 'active movement'. The peak velocity was found by performing a division of the active movement length by the active movement duration. The percentage of events refers to the the number of puncta moving actively relative to the total number of puncta. Compartment area and mean fluorescence intensity were determined using the free hand selection tool in ImageJ. Intensity values were obtained from images pre-edit.

Drug injection

Embryos were dechorionated and glued to a coverslip using heptane glue. The embryos were dehydrated for 12–15 min, covered in Halocarbon oil 700 (Sigma), and injected with colchicine or water. After injection, the embryos were placed on an air-permeable membrane and imaged on the spinning disk confocal microscope.

Statistics and Repeatability

Statistical significance was tested for using Student's t-test unless otherwise stated. *ns*: $p>0.05$; *:$p<0.05$; **: $p<0.005$; ***: $p<0.0005$. Error bars indicate standard error. All quantified values were from, at minimum, 3 embryos.

RESULTS

Furrow dynamics in wild type embryos

Measuring membrane length over time has provided insight into the dynamics of membrane furrow formation during the creation of an epithelial sheet in *Drosophila* development (Xie and Blankenship, 2018). Here, using transgenic flies with GFP tagged Resille (membrane marker) and RFP tagged Histone2A (chromosomal marker), I see the same trends that have previously been reported. True furrows were defined as the length of membrane that extends from the base of the apical caps to the end of the furrow canal, and cycle times were aligned with furrow measurements using the Histone:RFP marker. The furrows in each cycle reach their maximum length at the onset of anaphase before retracting. In cycle 10, furrows reach about 1.5 μm and the furrows in cycle 11 reach about 2 μm. Cycles 12 and 13 have a distinct second ingression phase which allows the furrows to lengthen to 5.5 μm and then 8 μm, respectively (Figure1A and B). In addition to furrow depth increasing, the cell borders were observed to become more distinct and regular with each progressive cycle (Figure 1C). The cycles get progressively longer as well, with cycle 10 lasting approximately 9 minutes and cycle 13 lasting about 20 minutes.

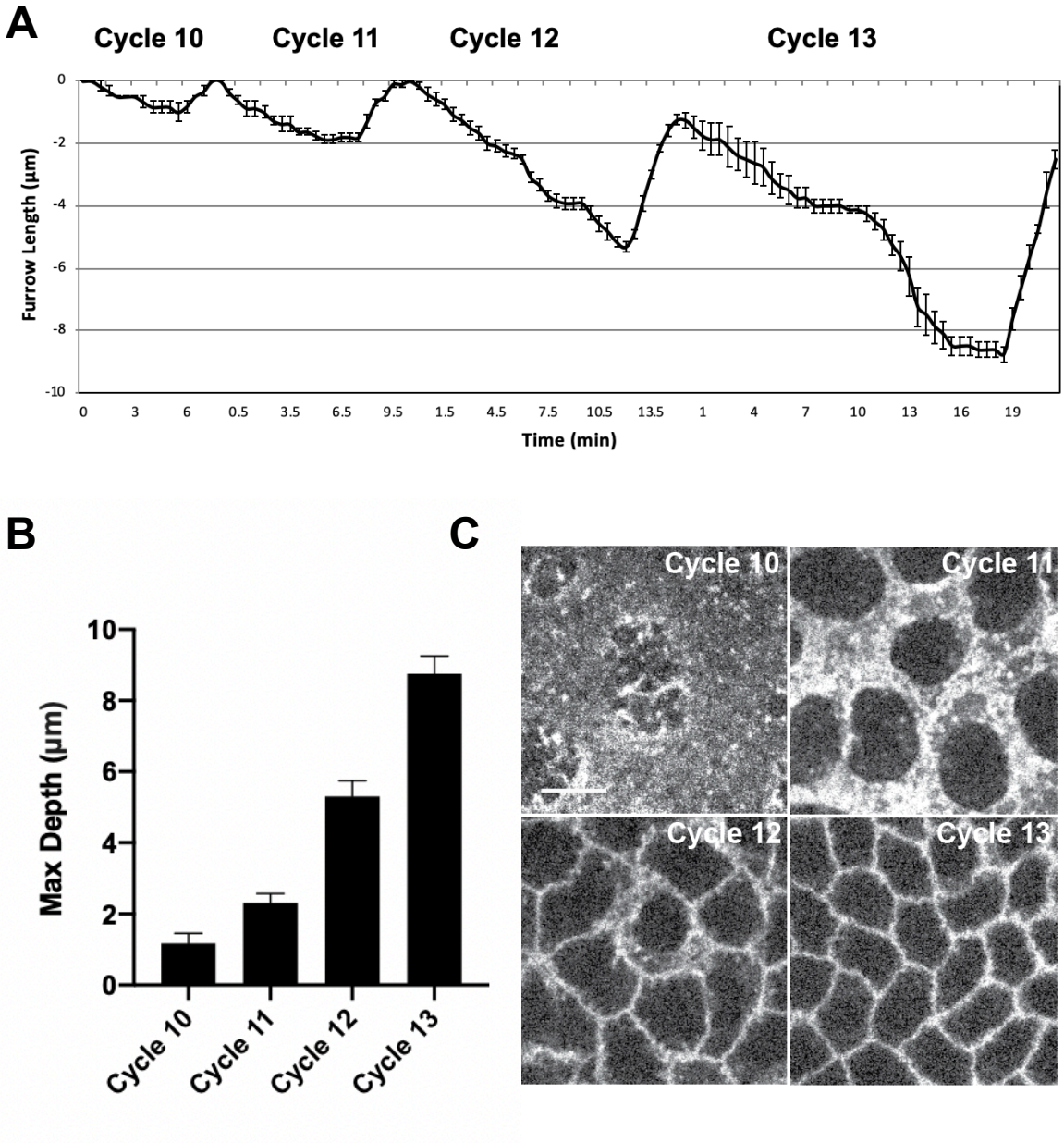

Figure 1. Dynamic furrow behaviors during syncytial cycles 10-13. (A) Furrow dynamics of control embryos expressing Resille:GFP from syncytial cycles 10-13 (Cycle 10: n=3, Cycle 11 and 12: n=5, Cycle 13: n=4). (B) Maximal furrow depths at onset of anaphase in cycle 10-13 (C) Still images of the change in membrane shape in each of the 4 cycles. Scale bar = 10µm.

Golgi-derived membrane as a source for furrow ingression

In the developing *Drosophila* embryo, there are multiple pools from which it can draw from in order to obtain the membrane necessary for furrow ingression. Previous work has shown that these pools include both endocytic and exocytic vesicles, as well as vesicles originally based from the Golgi (J.C. Sisson et. al., 2000). Although this work implicates Golgi-based vesicle delivery in the successful creation of a membrane furrow, a comprehensive look at Golgi dynamics at the beginning of this process (syncytial cycles 10-13) has not been conducted. I thus wanted to determine how Golgi dynamics change during furrow formation, and I observed that large Golgi compartments congregate in the cortex of the embryo and remain very static until cycle 10 begins. As soon as the nuclei migrate to the periphery of the embryo and membrane furrows begin to form, the compartments become much more dynamic and motile, with tubules occasionally extending and retracting from them. With each progressive cycle, the compartments become smaller and less numerous (Figure 2A). The average area decreases from 4.6 +/- 0.82 to 1.84 +/- 0.54 microns squared from cycle 10 to cycle 13, and the number of puncta in a 5 micron by 5 micron area is reduced from 32 +/- 2.35 to 10 +/- 1.15 (Figure2B and C) The shrinking of these compartments coincides with the progressive lengthening of membrane furrows, suggesting that they are acting as a reservoir of membrane needed to complete ingression.

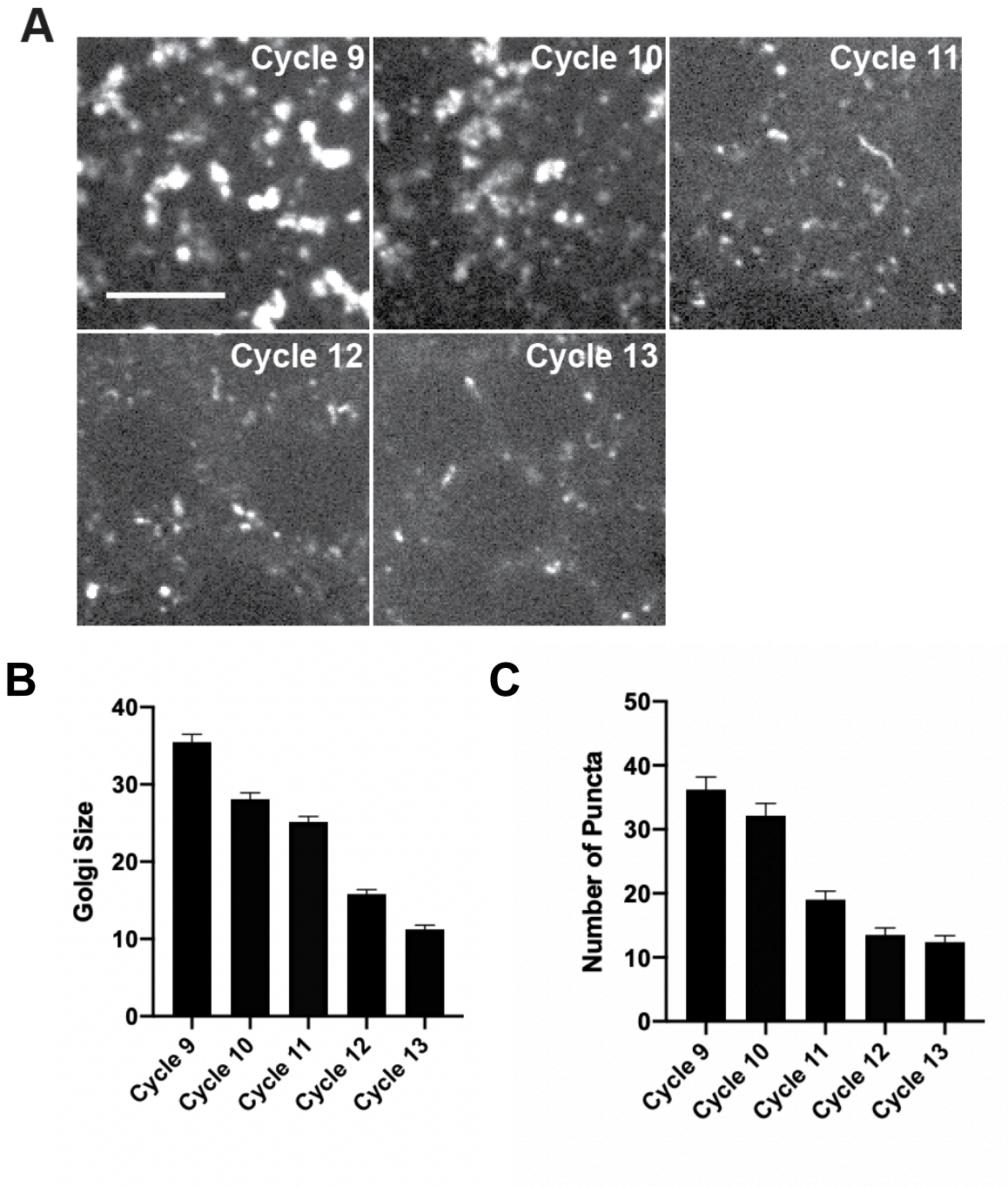

Figure 2. Golgi dynamics during syncytial cycles. (A) Still images from embryos expressing the Golg omarker RFPGALT during cycles 9, 10, 11, 12, and 13. Scale bar=10μm. (B) Quantification of average Golgi compartment area (in pixels) in each cycle 13 (Cycle 9: n=363, Cycle 10: n=291 Cycle 11: n=192, Cycle 12: n=120, Cycle 13: n=114) (C) Quantification the number of Golgi compartments in each cycle. (n=15)

Rab39 demonstrates a dynamic localization with trans-Golgi compartments

Given that Rab39 has previously been shown to localize on the Golgi, I wanted to further explore the behaviors of Rab39 with this organelle during syncytial furrow formation. (D'Souza et al, 2019)(Chen et al, 2003). Embryos expressing Rab39:YFP and GALT:RFP (Golgi marker) were used to track the actions of Rab39 and the Golgi. Not surprisingly, the two show a striking colocalization. Rab39 and Golgi marked compartments were very motile and dynamic in shape, with long tubule like projections occasionally protruding and then receding (Figure 3C). In order to determine whether Rab39 localizes specifically to the cis or the trans-Golgi, antibody stains were conducted. Endogenous Rab39 as well as Golgin-245 (trans-Golgi marker) or Lava Lamp (cis-Golgi marker) were stained for. These revealed that Rab39 colocalizes with Golgin-245, but not with Lava Lamp. Together, the live and fixed imaging results suggest that Rab39 has a close, dynamic relationship to the trans-Golgi.

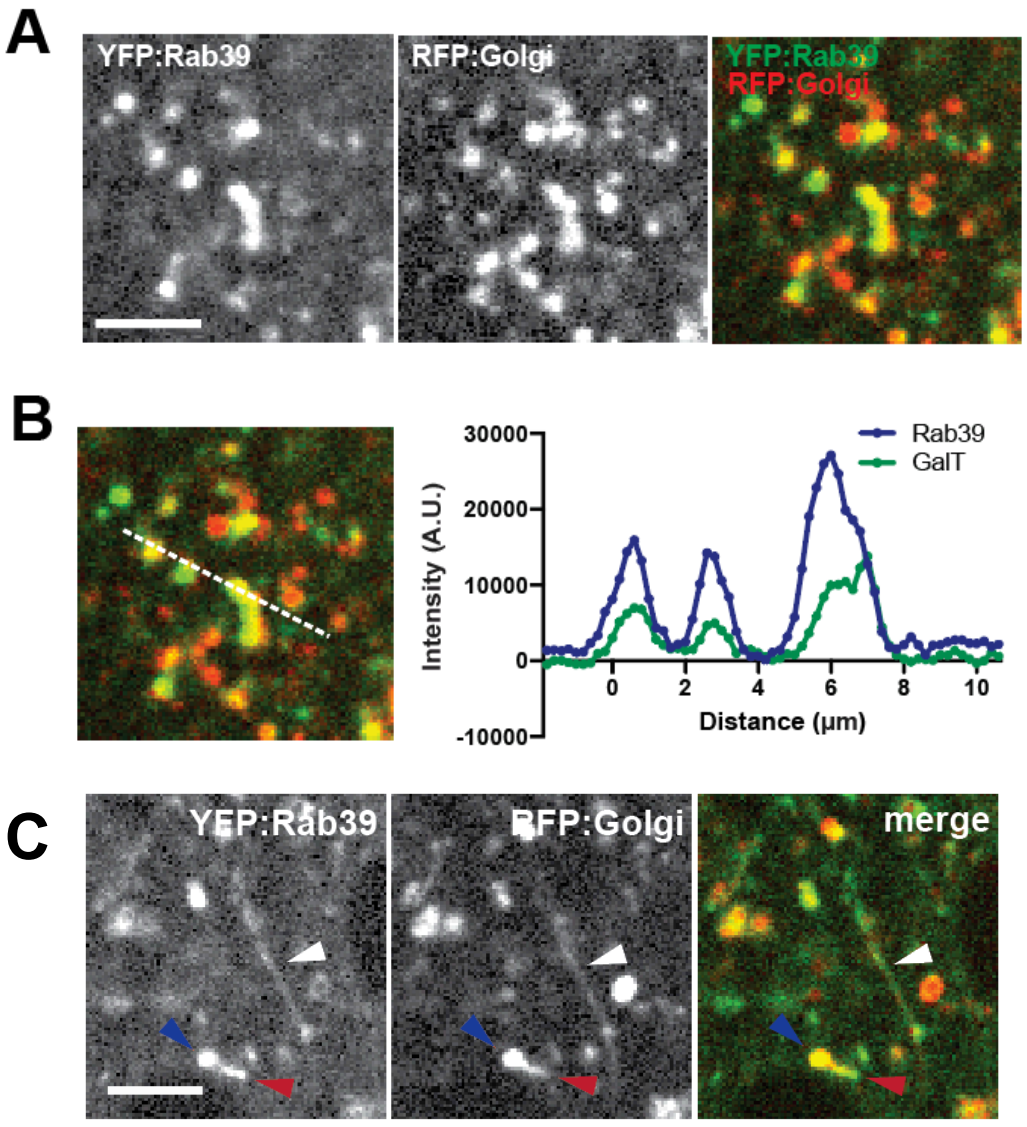

Figure 3. Rab39 is localized to the trans-Golgi and demonstrates similar dynamics. (A) Still images from embryos expressing YFPRab39 and the Golgi marker RFPGALT. (B) Colocalization of Rab39 and GALT mapped by intensity values of each channel across 10µm. (C) Dynamics of Rab39 and Golgi. Compartments can take the form of puncta (blue arrows), short (red arrows) and long (while arrows) tubules. Scale bars=5µm.

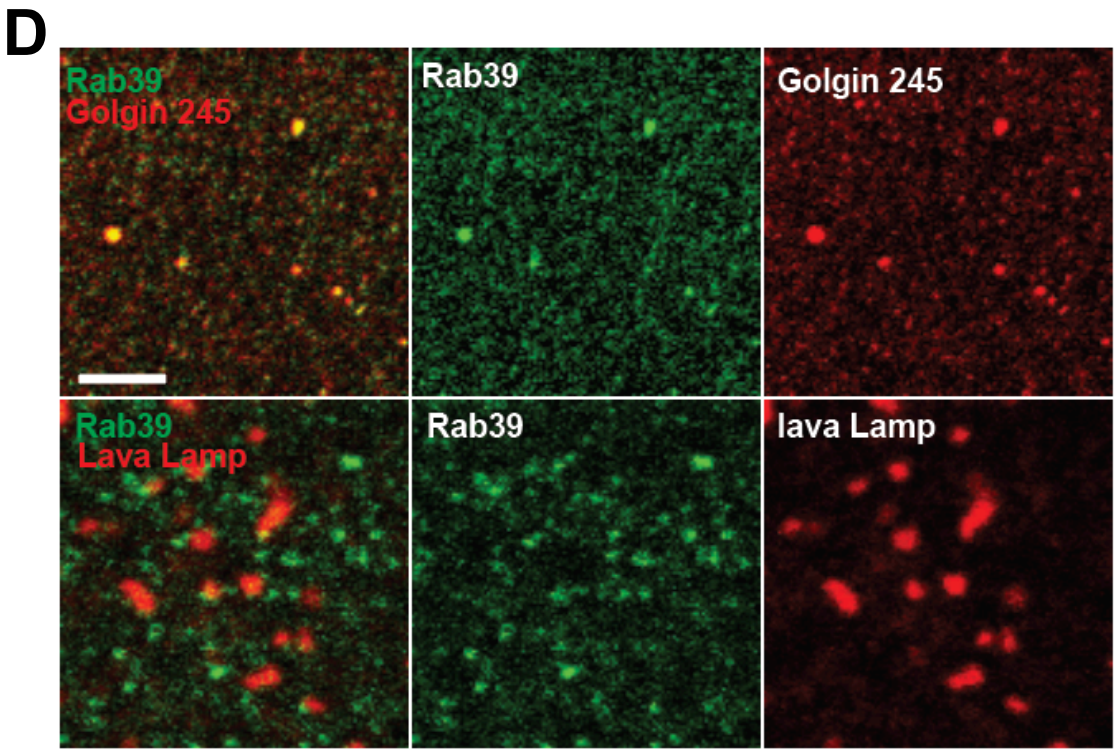

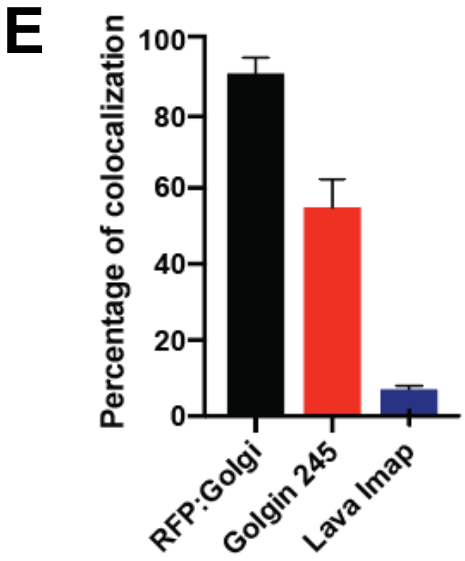

Figure 3 continued. Rab39 is localized to the trans-Golgi and demonstrates similar dynamics. (D) Fixed embryos expressing endogenous Rab39GFP stained for Rab39 and Golgin245 or Lava Lamp. Scale bar=5µm. (B) Percent Golgi puncta colocalized with Rab39 puncta. (n ≥ 3 embryos). Images and data analysis by Hui Miao.

Rab39 is required for syncytial furrow ingression

In order to investigate the role of Rab39 during early embryogenesis, I used an shRNA line targeting Rab39 mRNA to knock down Rab39 expression in the embryo. Imaging embryos expressing the Rab39shRNA as well as a membrane marker (Resille:GFP) revealed that furrow ingression is significantly reduced with Rab39 knockdown. The membrane furrows in each cycle only lengthen to about 2 microns before receding. This makes the difference most apparent in cycles 12 and 13, where Ingression II is totally abolished (Figure 4A and B). This could be due to the fact that Ingression II is driven by the transition to zygotic transcription, where the maternal contribution of Rab39 allows the furrows to ingress to 2 microns, but mRNA transcripts produced by the embryo beginning cycle 12 are targeted for degradation with the shRNA. Cycle times are also shorter in disrupted embryos by several minutes (Figure 4A). This could be because disrupting Golgi traffic with Rab39shRNA not only stops membrane supply via Golgi-mediated vesicle addition, but also stops the distribution of cytokinetic regulatory proteins (Drechsel et al, 1997)(Altan-Bonnet, 2003).

The defects in furrow ingression result in failures of mitosis, where mitotic collapse or the fusion of adjacent nuclei can occur (Holly et al, 2015). The resultant polyploid nuclei fall out of the cortex of the embryo into the yolk, causing the cell boundaries to shrink in size creating “mini-cells” (Figure 4C). The high level of nuclear fallout results in many less nuclei populating the cortex of the embryo than what would

be predicted for that cycle. By cycle 13, only 56.43 +/- 9.95% of nuclei predicted for that cycle remain in the cortex (Figure 4D). The multiple defects during furrow formation seen with the reduction of Rab39 suggest that it is an important regulator in the directed traffic of membrane in cytokinesis.

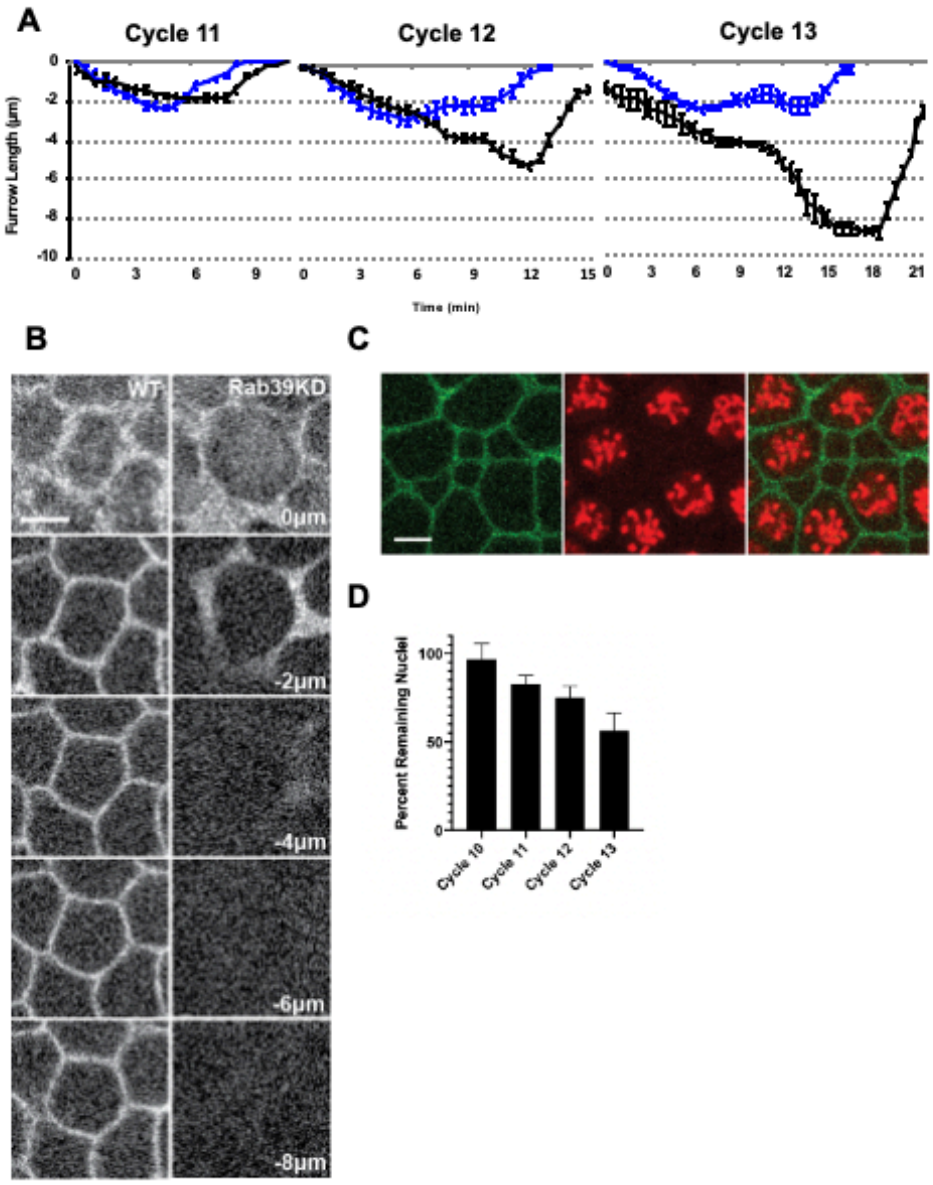

Figure 4. Knockdown of Rab39 with shRNA causes furrow defects. (A) Furrow dynamics of control (black) and Rab39shRNA (blue) embryos from syncytial cycles 11-13 (Rab39shRNA: Cycle 11: n=5, Cycle 12: n=6, Cycle 13: n=5 ; Control: Cycle 11 and 12: n=5, Cycle 13: n=4). (B) Difference in maximal furrow depths at cycle 13 in Rab39 knockdown embryos (117GFP). z=0µm is the apical surface and z=8µm is the most basal. Scale bar=5µm. (C) Still images of cell shape abnormalities caused by nuclear fallout. (117GFP, HistoneRFP). Scale bar=5µm. (D) Quantitative analysis of nuclear fallout after each indicated cycle represented as the percentage of nuclei that are observed after each division compared to the predicted number.

Movement of Rab39 and Golgi compartments is microtubule-dependent

Observing the dynamic movements of Rab39 raises the question of how it travels throughout the cell. Being that the movement of many organelles and vesicles is mediated by microtubule scaffolding, I decided to explore this possibility. Inhibiting the polymerization of microtubules with colchicine decreases the motility of Rab39 and Golgi compartments (Figure 5A and B). The average velocity of all selected compartments, indicated as the absolute velocity, is reduced from about 2 μm/minute in control embryos to less than 1 μm/minute in colchicine injected embryos (Figure 5E). In each population of compartments, there is a subpopulation that is more motile (moving more than 5 pixels in 10 seconds). The percentage of compartments that meet these criteria falls from about 30% in control embryo to 5% in colchicine injected embryos (Figure 5D). In addition, the velocity of these "active" vesicles decreased with colchicine injection. The peak velocity in control embryos is about 0.6 μm/second, where it is 0.1 μm/second in treated embryos (Figure 5F).

The decrease in movement seen with Rab39 and the Golgi when microtubule polymerization is inhibited indicates that the trafficking of these vesicles is microtubule dependent. Knowing that this movement is microtubule dependent not only provides further insight into how this pathway delivers excess membrane to furrows, but also what types of proteins may be Rab39 effectors.

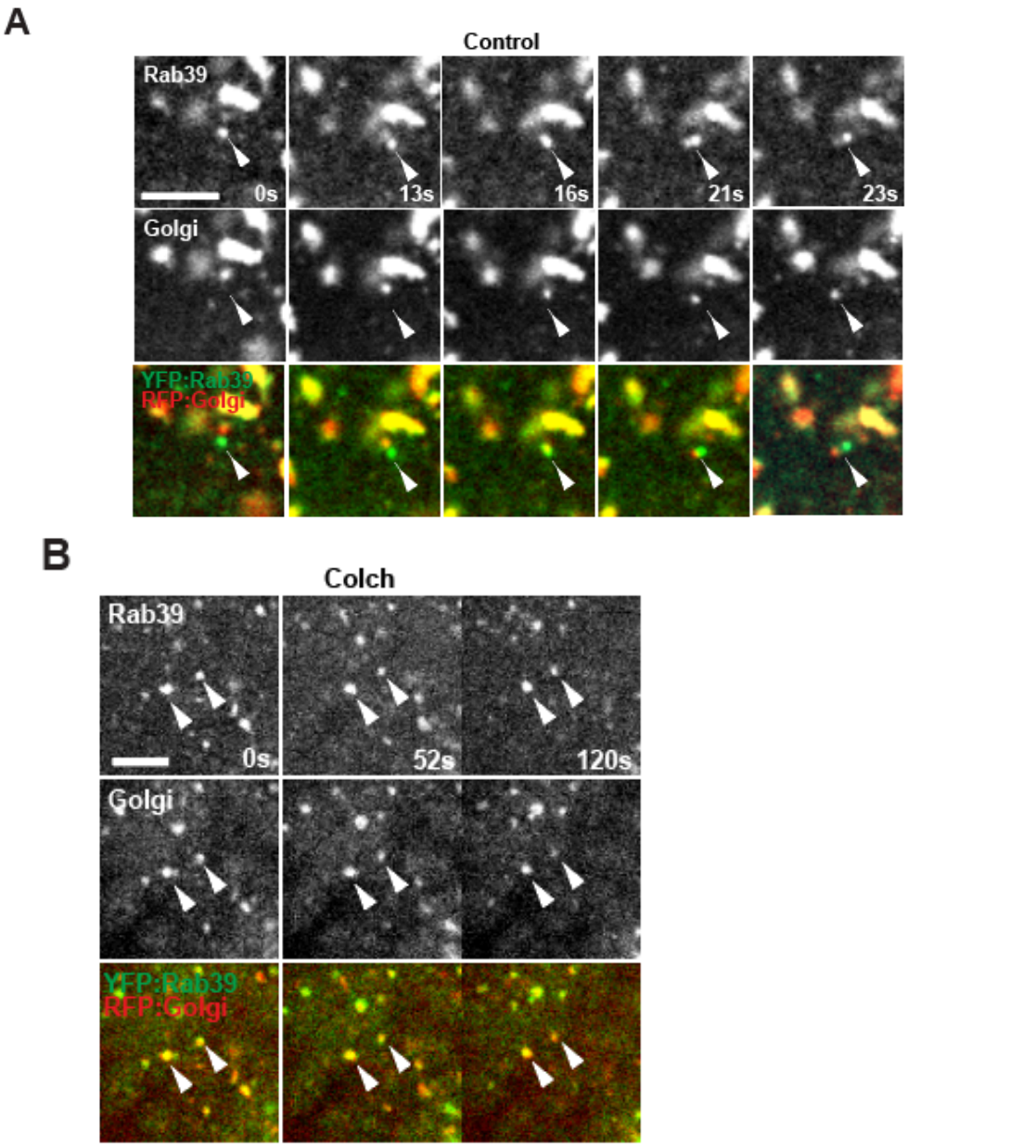

Figure 5 continued. Microtubule inhibition decreases Rab39 and Golgi motility. (A and B) Time points from live imaging of YFP:Rab39 and RFP:GALT showing the movement of Rab39 and Golgi compartments in control and colchicine injected embryos. Scale bar=5µm.

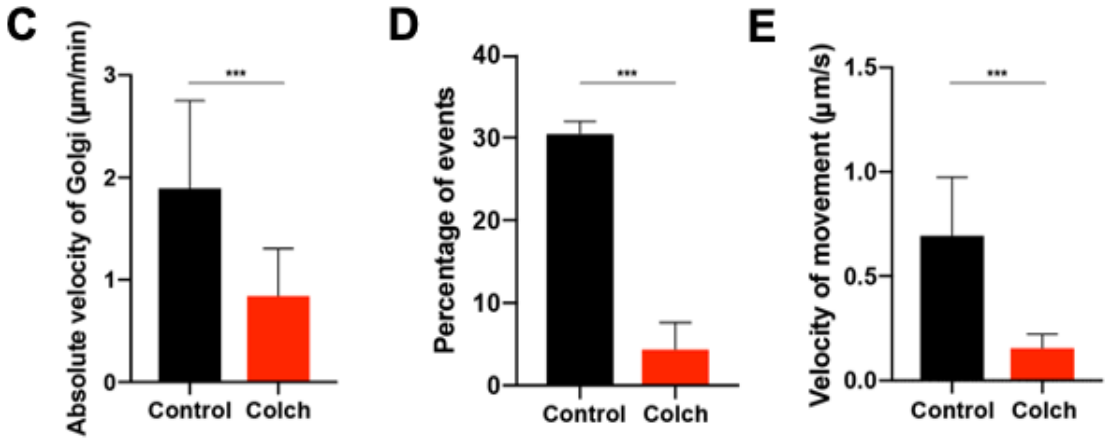

Figure 5 continued. Microtubule inhibition decreases Rab39 and Golgi motility. (C) Absolute velocity of Golgi compartments in control and colchicine injected embryos. (D) Percent of Golgi compartments that displayed rapid movement in control and colchicine injected embryos. (E) Velocity of Golgi compartments that demonstrated rapid movement. Mann-Whitney U test. Images and data analysis by Hui Miao.

Kinesin-3 family member Klp98A is also required for syncytial furrow ingression

Knowing that the movement of Rab39 and Golgi compartments is microtubule dependent, and that motor proteins are often effectors of Rabs, I began to search for a potential effector of Rab39. Rab GST-Rab Affinity Chromatography has revealed that the kinesin-3 family member unc-104 as a potential effector of Rab39. (Gillingham et. al. 2014) This data led me to look at another Kinesin-3 family member, Klp98A (Kinesin-like protein at 98A), as a potential effector.

To see if knocking down Klp98A produced similar defects as knocking down Rab39, I used another shRNA line targeting Klp98A. I observed that the knockdown of Klp98A results in the abolition of furrow formation, indicating that it is important for this process as well (Figure 6A and B). In addition to furrow defects, nuclear fallout was also seen as a result of failed divisions. This nuclear fallout leads to a similar "mini-cell" phenotype that is seen in Rab39 knockdown embryos (Figure 6C). By cycle 13, 68.36 +/- 12.06 of nuclei expected for that cycle remained in the embryonic cortex (Figure 6D). The similar phenotypes seen with Klp98A shRNA signify that this motor protein is essential for membrane addition during furrow formation and may be involved in the same pathway as Rab39.

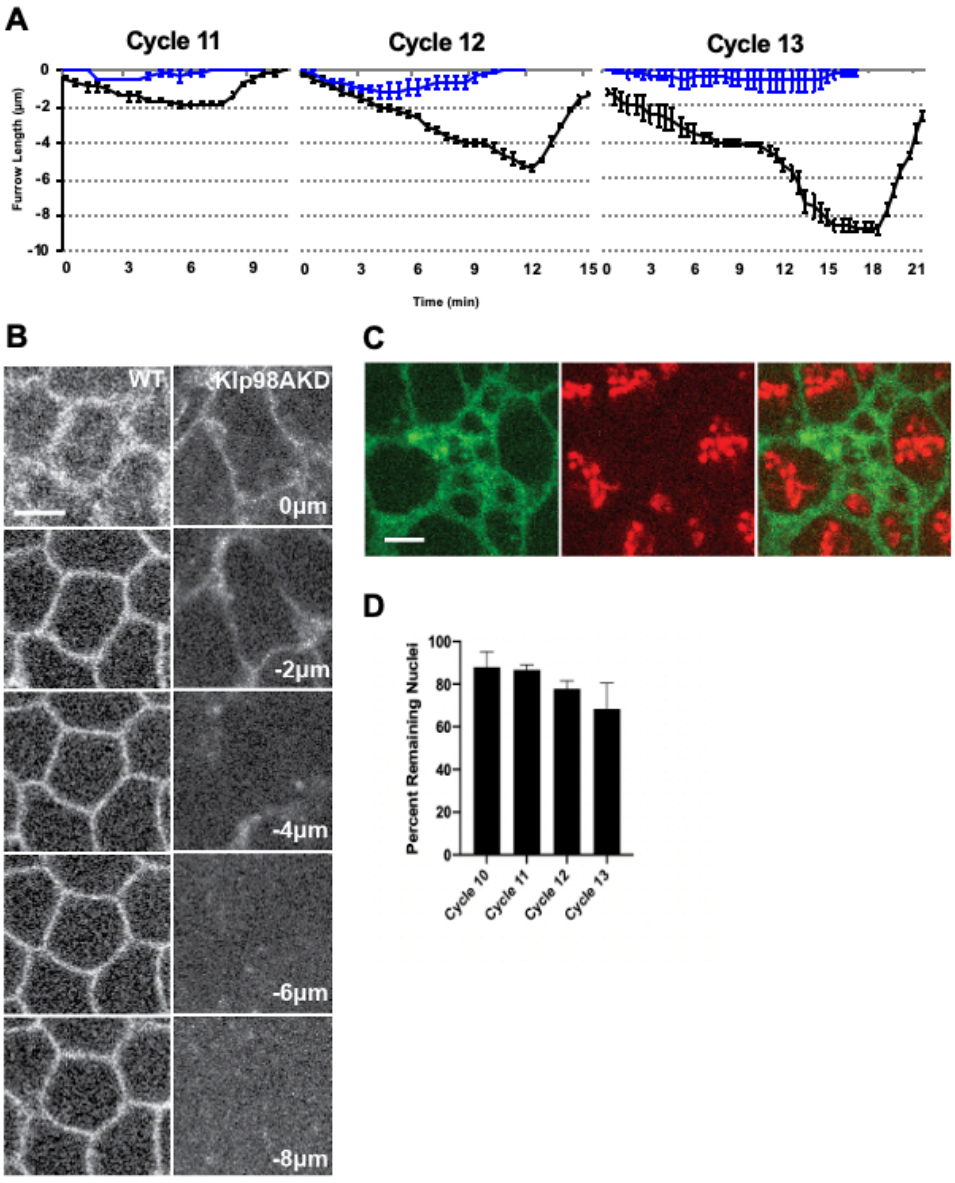

Figure 6. Knockdown of Klp98A using shRNA produces similar defects in furrow formation. (A) Furrow length measurements over time of control (black) and klp98AshRNA (blue) embryos from syncytial cycles 11-13 (Klp98AshRNA: Cycle 11: n=3, Cycle 12: n=6, Cycle 13: n=4 ; Conrol Cycle 11 and 12: n=5, Cycle 13: n=4 embryos). (B) Still images of embryos expressing 117GFP and their maximal furrow length depth during cycle 13. Scale bar=5µm. (C) Still images of cell shape abnormalities caused by nuclear fallout. (D) Percent nuclei remaining after each nuclei compared to the predicted amount

Klp98A as a downstream effector of Rab39

To further explore Klp98A as a potential effector of Rab39, I performed antibody stains for endogenous Rab39 and Klp98A. During cycle 12, at 6 μm below the apical surface, 54.80 +/- 7.45% of Rab39 puncta are colocalized with Klp98A puncta (Figure 7A and B). The ratio of colocalized puncta decreased above and below 6 μm (Figure 7B). This may be because furrows reach a maximum length of just under 6 μm in cycle 12, and the Golgi has been shown to localize to ingressing furrows (Sission et al, 2000).

If Klp98A is in fact a downstream effector of Rab39, then knocking Rab39 down should produce some change in Klp98A. Indeed, when Rab39 shRNA embryos are stained for Klp98A a drastic difference is observed. Klp98A puncta go from being small and diffuse in control embryos to large and concentrated near the nucleus in Rab39 shRNA embryos (Figure 7C). Staining the DNA and nuclear envelope with DAPI and anti-lamin reveals that there are large chromosomal fragments that have disassociated from the nucleus outside of the nuclear envelope. These fragments could arise during mitotic failures caused by furrow defects in these embryos. Klp98A in this knockdown background relocalizes specifically to these large chromosomal fragments, however, it is still unclear how or why this occurs. The evidence that Klp98A not only colocalizes with Rab39, but also is redistributed in the absence of Rab39 makes it a strong candidate for a Rab39 effector.

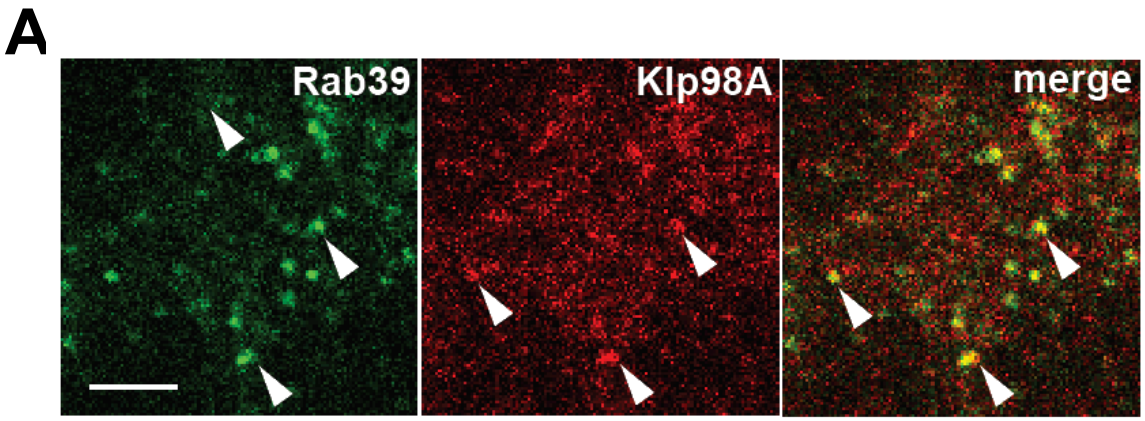

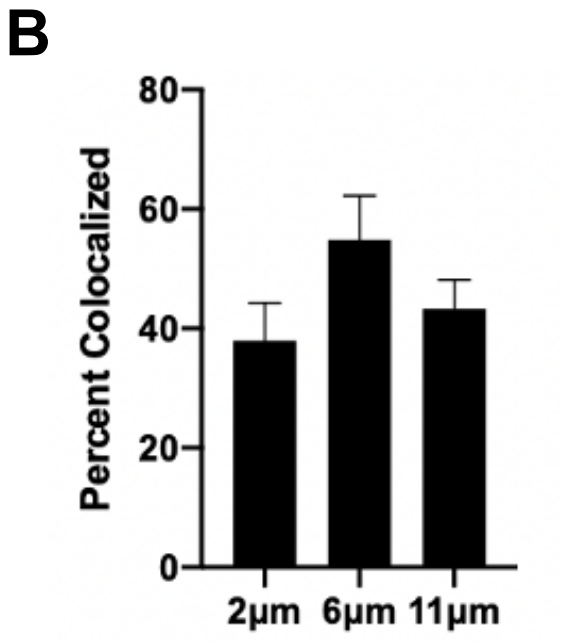

Kinesin 3 family member Klp98A. (A) Fixed embryos expressing endoRab39GFP stained for Rab39 and Klp98A. Scale bar=5µm. (B) Percent Rab39 puncta colocalized with Klp98A puncta at 2, 6, and 11µm below the apical surface (2µm n=95, 6µm n=92, 11µm n=111 puncta).

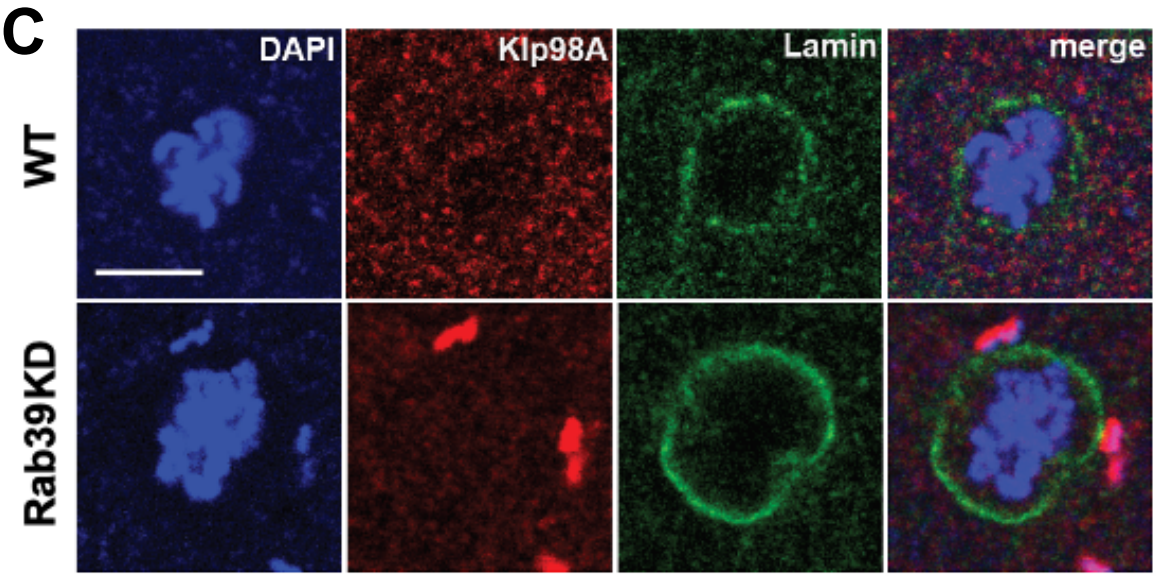

Figure 7 (continued). Rab39 directly interacts with Kinesin 3 family member Klp98A. (C) Fixed embryos stained for DAPI (blue), Klp98A (red), and Lamin (green) in control (OreR) and Rab39shRNA embryos showing the change in klp98A puncta. Scale bar=10μm.

Rab39 controls Golgi size during syncytial development

In order to begin to connect these proteins back to Golgi-based membrane delivery during furrow formation, I wanted to see how the Golgi would behave when Rab39 levels are impacted. If Rab39 is truly involved with Golgi-mediated membrane addition, then some change in Golgi structure should be observed when Rab39 is diminished. Rab39shRNA causes a decrease in both Golgi size and number, whereas Rab39 overexpression causes an increase in both (Figure 8A, B and C). The difference in size was more significant than the change in number in both groups. These data suggest that Rab39 is involved with directing traffic of vesicles to the Golgi, sequestering enough excess membrane to be used during furrow formation.

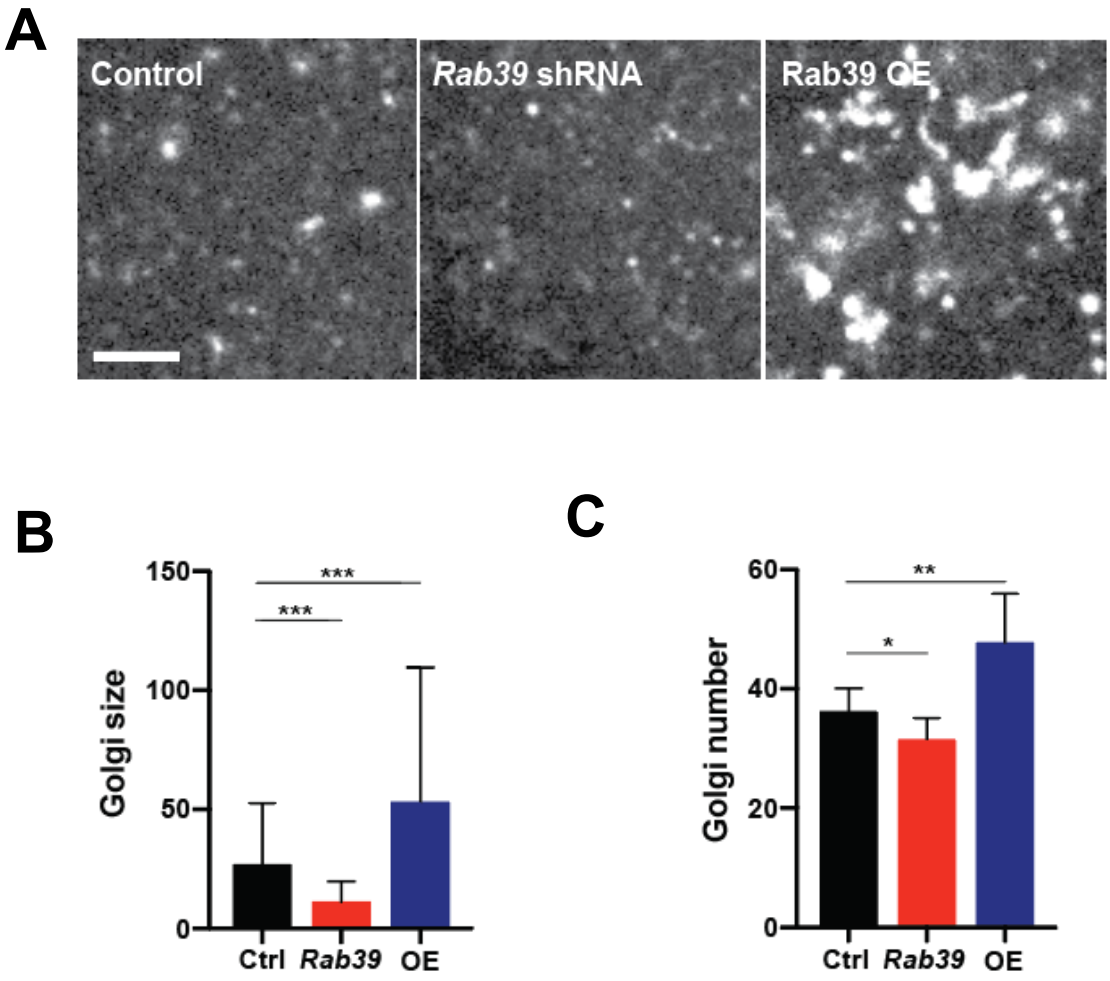

Figure 9. Rab39 controls Golgi size during syncytial development (A) Still images from embryos expressing RFP:GALT (Golgi marker) in Rab39 shRNA or overexpression conditions. Scale bar=5µm. (B) Quantification of Golgi size in Rab39 shRNA or overexpression conditions in pixels (C) Count of the number of Golgi compartments found across the different expression levels. Scale bar=5µm. Images and data analysis by Hui Miao.

Klp98A controls Golgi movement and dynamics

To look at the behaviors of the Golgi when Klp98A is depleted, Golgi compartments were live imaged in Klp98A shRNA embryos. If it is a motor protein that mediates the movement of Golgi vesicles, this should have similar effects on Golgi motility as inhibiting microtubule polymerization with colchicine. Not only was there a change in motility, there were also changes to Golgi shape dynamics.

Klp98A shRNA reduced the ratio of compartments that were motile, the average velocity, and the peak velolcity (Figure 9F, G, H), albeit less so than colchicine injection. This is most likely due to Klp98A shRNA being merely a knock down of this one motor protein, instead of the total inhibition of microtubule activity. Another phenotype was observed related to Golgi morphology. Klp98A shRNA increased the duration and maximum length of tubules emanating from Golgi compartments, but not overall size. Tubules in control embryos usually retracted within 20 seconds, whereas tubules in Klp98A shRNA embryos lasted over one minute (Figure 9C and D). These tubules displayed a "wandering" phenotype, where they moved about in multiple directions as they lengthened, rather than being straight and concise (Figure 9A and B). These results suggest that Klp98A has an important role in mediating the direct trafficking of Golgi membrane to ingressing furrows.

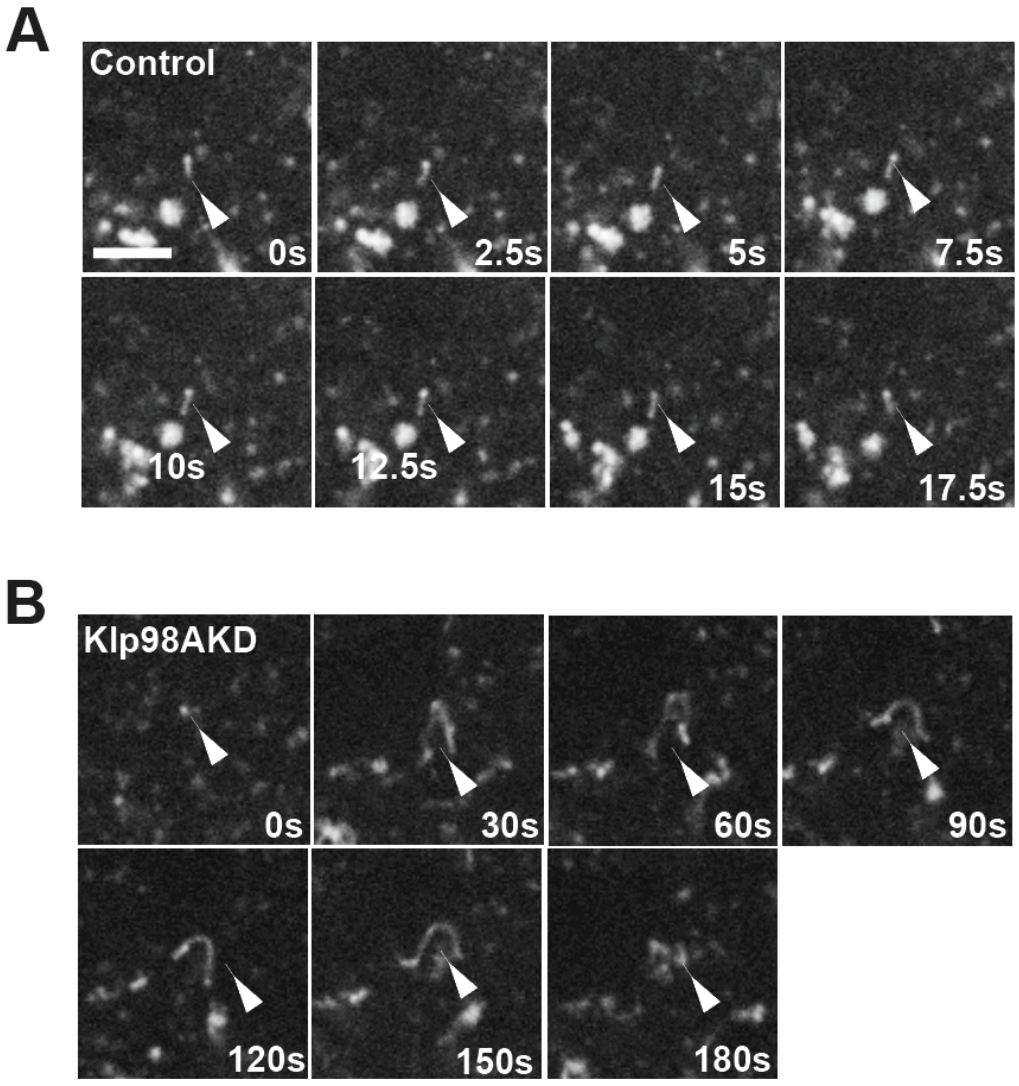

Figure 9. Knockdown of Klp98A causes an increase in Golgi tubule length and duration. (A) Still frames from movies capturing the lifetime of a Golgi tubule (arrows) in control and Klp98A shRNA (B) embryos. Scale bar = 2.5 μm

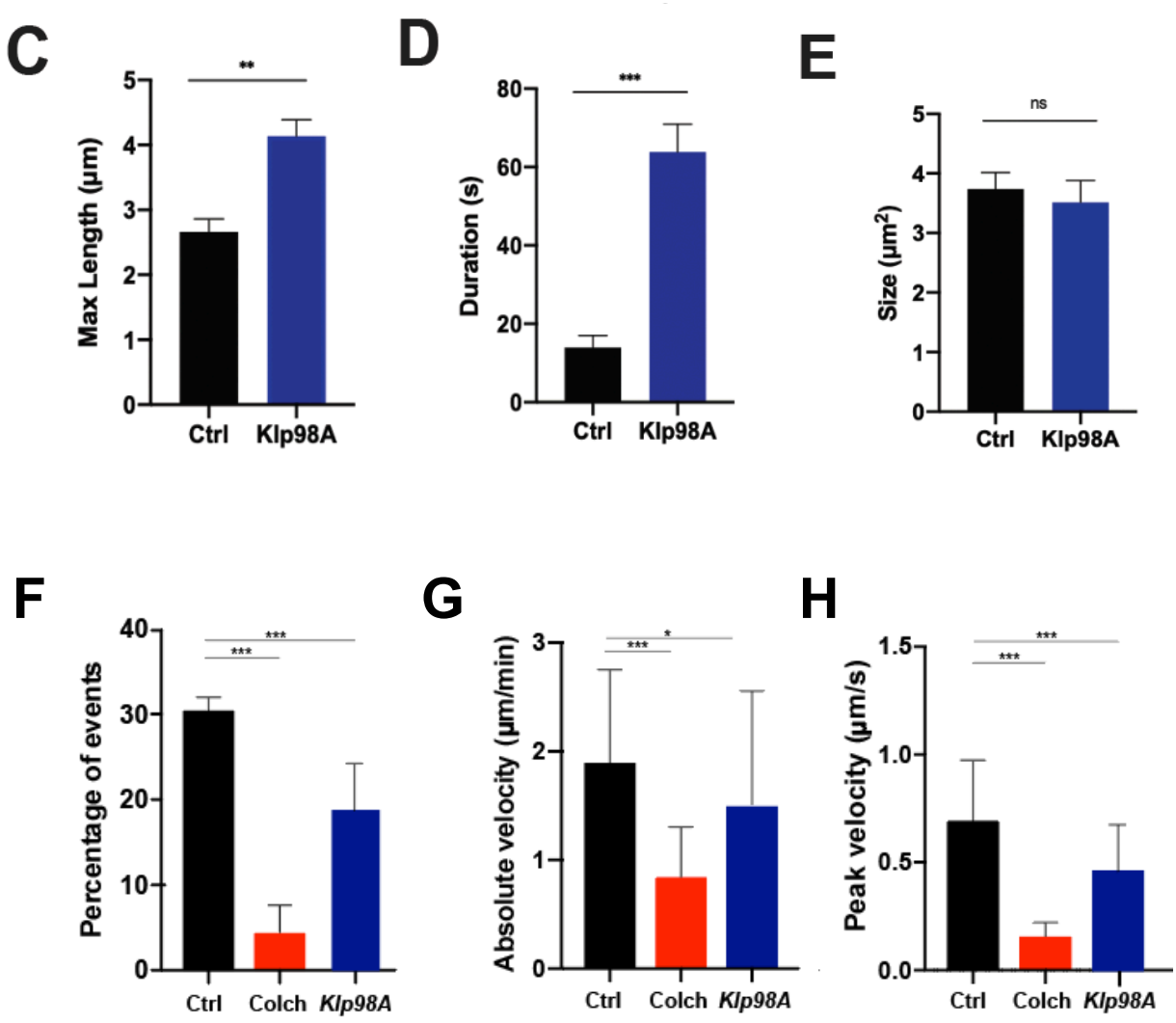

Figure 9 continued. Knockdown of Klp98A causes an increase in Golgi tubule length and duration. (C) Quantification of the maximum length reached by the tubule during its lifetime and (D) the overall duration of the tubule. (E) Area of Golgi puncta in control and Klp98A shRNA embryos. (Klp98AshRNA: n=51 Control: n=15) (F) Absolute velocity of Golgi compartments in control and Klp98A shRNA embryos. (D) Percent of Golgi compartments that displayed rapid movement in control and Klp98A shRNA embryos. (E) Velocity of Golgi compartments that demonstrated rapid movement. Mann-Whitney U test.

Acto-myosin networks depend on membrane addition for proper distribution

In addition to membrane addition, acto-myosin contractility is an indispensible aspect of cytokinesis and furrow formation, as it generates the necessary force to undergo these cell and tissue morphology changes. (He et al 2016). To determine whether the targeted addition of Golgi membrane is necessary for proper actin and myosin localization, I live imaged actin and myosin in Klp98A and Rab39 disrupted embryos. To look at actin, I used embryos expressing Moesin:GFP, which is a protein that links the actin cytoskeleton to the plasma membrane. In control embryos, actin normally localizes to the apical surface above the nuclei, as well as all along ingressing furrows down to their leading edges (Figure 10A). However, in Klp98A depleted embryos, actin seems to stay localized only to the apical caps (Figure 10A). Even at the apical surface, actin organization differed in Klp98A shRNA embryos, reflected by the intensity of the Moesin:GFP being significantly reduced compared to control embryos (Figure 10B). Myosin displays a different distribution in the syncytial blastoderm, where it localizes only to the bases of membrane furrows (He et al 2016). To look at Myosin distribution, embryos expressing Spaghetti Squash:GFP (spsqh), which marks Myosin II regulatory light chain, were used. With this marker I observed that Myosin still was recruited to the leading edge of these furrows in Rab39 shRNA embryos, however at much lower levels. The average Spgsqh:GFP intensity was decreased significantly compared to control embryos (Figure 10B and C). Actin and Myosin distributions being impacted by Rab39 pathway disruption indicates that the addition of Golgi-derived membrane is essential to the proper recruitment and localization of these force-generating components. It is

unclear still if this is a result of there being directs cross-talk with this pathway specifically, or if membrane addition in general is required for the correct distribution of these contractile elements.

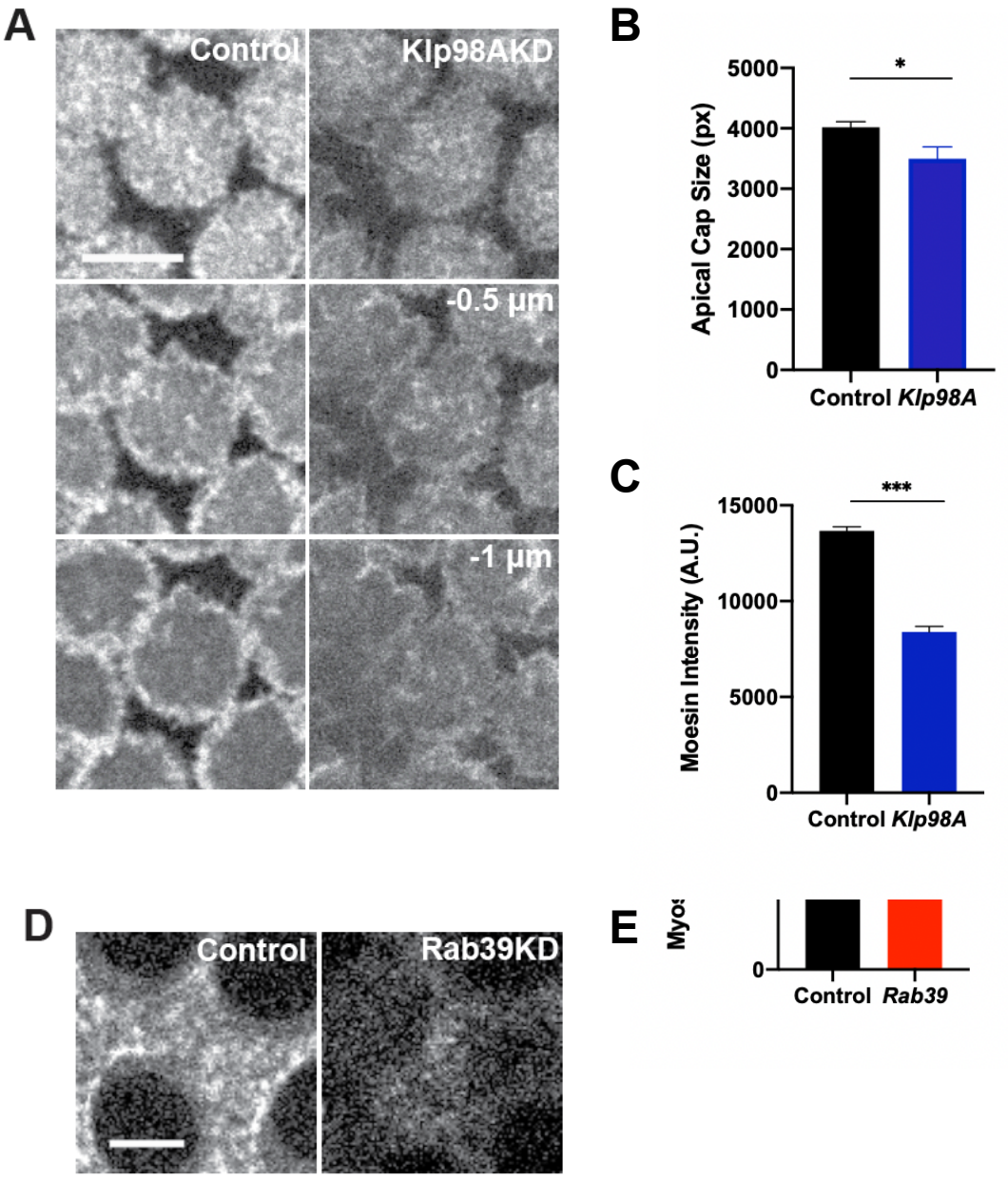

Figure 10. Disruption of the Rab39 pathway hinders actin and myosin distribution. (A) Still frames capturing actin localization using Moe:GFP in control and Klp98A disrupted embryos. Scale bar =10 µm (B) Quantification of apical cap area and (C) Moesin intensity. (n=14) (D) Still frames capturing myosin localization with Spsqh:GFP in control and Rab39 shRNA embryos. Scale bar =5 µm (E) Measurements of myosin intensity in 15 x 15 pixel areas.

DISCUSSION

Overall Conclusions

The work here has revealed that Rab39 is required for membrane addition to ingressing syncytial furrows in the syncytial *Drosophila* blastoderm. Rab39 is localized on trans-Golgi compartments and is important for forming a complete membrane furrow during early *Drosophila* embryogenesis, as disrupting it using RNA interference results in shallow membrane furrows, polyploid nuclei from mitotic collapse, and nuclear fallout as a result of these nuclear abnormalities (Figure 3, 4). Golgi size is impacted by Rab39 expression, indicating that it is important for the sequestration of membrane in this organelle (Figure 9). Rab39 displays dynamic tubules that may be driven by the motor protein Klp98A, which is also crucial to the development of a complete membrane furrow and shows similar phenotypes to Rab39 when perturbed (Figure 6). The movement of these dynamic tubules is dependent on microtubule networks, as inhibition of microtubule polymerization with colchicine decreases compartment mobility (Figure 5). The evidence of this relationship is further supported by the fact that the knockdown of Rab39 causes abnormalities in Klp98A and that these proteins are well colocalized. In wildtype embryos, Klp98A puncta are small and diffuse, but in the absence of Rab39 the puncta drastically increase in size and intensity (Figure 7).

Rab39 as a regulator of furrow ingression

In the formation of an epithelial sheet, cell division and consequently proper cell arrangement and density rely on membrane furrows physically separating neighboring nuclei. With each division, the risk of mitotic failures increases if furrows do not effectively aid in separation. Previous work has indicated that there is an inverse relationship between furrow length and these mitotic defects (Xie and Blankenship 2018)(Holly et al, 2015). In Rab39 deficient embryos, where furrows do not ingress past ~2 μm, missegregation events result in morphological defects in the developing epithelium.

Successful furrow ingression in wild type embryos occurs in two phases, Ingression I and Ingression II, separated by a Stabilization period, where Ingression II is driven by the transition from maternal to zygotic gene transcription (Xie and Blankenship, 2018). Interestingly, Rab39 knockdown disrupts this biphasic nature, as it mainly affects Ingression II. The embryo is thus dependent on the zygotic contribution of Rab39 in order to complete Ingression II (Figure 4). In wild type embryos, Ingression II also affects the morphology of furrows, where they go from being more broad and disorganized to narrow and regular (Figure 1). In addition to furrow defects, Rab39 depleted embryos display furrows that do not become as sharp as control embryos, although there is some organization from cycles 10-13 (Figure 4). When missegeration events occur in these embryos, the defective nuclei fall out of the syncytium and the corresponding furrows maintain their structure, although they shrink to a fraction of their original size. The remaining furrow boundaries compensate for the difference in size and

expand (Figure 4). This suggests that the cytoskeletal elements are still able to maintain some structural integrity at least near the apical surface. The data collected showing that actin only localizes on the apical caps and that myosin recruitment is impaired in Rab39 pathway disrupted embryos also support the idea that some cytoskeletal elements are retained, even if their organization is significantly impacted (Figure 10). Together, this data shows that Rab39 highly involved in furrow ingression, specifically in the addition of new membrane.

Rab39 mediates Golgi-dependent membrane furrow addition

To accomplish the creation of a membrane furrow, the cell must relocate membrane from internal pools (Albertson et al, 2005). The Golgi has previously been shown to be one of these pools, as disrupting Golgi function results in unsuccessful furrow ingression (Farkas et al, 2003), and Golgi vesicles have been observed relocating to the bases of ingressing furrows during *Drosophila* cellularization (Sisson et. al., 2000). Adding to this evidence, it was observed that Golgi vesicles become much more motile when furrow ingression begins, and that the size and number of Golgi compartments decreases drastically during cycle 10-13. The inverse relationship between Golgi size and furrow length indicates that excess Golgi membrane is being "used up" by furrows (Figure 2).

Rab39 demonstrates a dynamic colocalization with trans-Golgi compartments, where many different orientations are observed, including long tubules occiasionally emanating from the original circular compartment (Figure 3). In Rab 39 deficient embryos, not only did the furrows not ingress past ~2 μm, Golgi size was significantly

reduced. This would imply that Rab39 might be involved in recruitment of membrane from other sources to the Golgi intermediately before it is sent to furrows. Projections on the apical surface have been shown to be endocytosed and used for furrow ingression (Fullilove and Jacobson, 1971), and being that Rab39 has previously been shown to be involved in endocytosis (Chen et al, 2003), it is quite possible that Rab39 directs endocytic traffic to the Golgi.

Measuring the formation and retraction of furrows in Rab39 depleted embryos also revealed that the cycles are much faster than in control embryos (Figure 4). While this could be an indirect result of furrow abnormalities impacting other processes, it is also possible that it is directly related to Rab39's role in Golgi trafficking. The mitotic disassembly of the Golgi has been shown to not only be important for cleavage furrows in cytokinesis, but also necessary for the release and proper function of proteins needed for mitosis and cytokinesis. Diminishing Rab39 may also hinder the coordinated release of the proteins required for cell division, including mitotic regulatory proteins (Drechsel et al, 1997)(Altan-Bonnet, 2003). Together, this evidence points to Rab39 being a regulator of Golgi-dependent membrane addition during furrow ingression.

Klp98A directs excess Golgi membrane to furrows

In order for this excess membrane to be redirected from the Golgi to the lengthening furrow, it must be actively trafficked throughout the cell using cytoskeletal elements as scaffolding. The movement of Golgi and Rab39 compartments is specifically dependent on microtubule networks, as disruption of microtubule polymerization results in decreased compartment motility (Figure 3). This knowledge, as well as knowing Rab

effectors are often motor proteins, make microtubule motor proteins good candidates for Rab39 effectors. Klp98A is a Kinesin-3-family member, in which other members have been shown to have biochemical interactions with Rab39 (Gillingham et. al. 2014).

Klp98A shows partial colocalization with Rab39 and is also is necessary for proper furrow formation. Klp98A depleted embryos are unable to form furrows and behave somewhat similarly to Rab39 shRNA embryos, with furrows not ingressing past ~0.5 μm. Cycle times are shorter as well, which again may be an effect of disrupting Golgi traffic. Although Golgi size is not impacted by the absence of Klp98A, but the lifetime and length of the tubules that form is, as well as the overall movement of Golgi compartments. This change in shape and motility, as well as the changes to furrow dynamics, suggest that Klp98A is involved in the targeted trafficking of Golgi membrane to ingressing furrows.

Future Directions

To further understand how Rab39 sequesters and distributes membrane to and from Golgi compartments, it would be interesting to investigate the possible contribution of other membrane trafficking pathways. If a certain vesicle type is upstream or downstream of Rab39 and required for this membrane sequestration and distribution, it would be expected that there would be changes to vesicle size and distribution in Rab39 shRNA embryos, and vice versa. Some potential markers that could be used to screen for phenotypes are Rab4 and Rab5 to look at early endosomes, Rab7 to look at late endosomes, Rab35 and Rab11 to look at recycling endosomes, and Rab8 to look at exocytic vesicles.

In addition, in order to get a bigger picture of Rab39's interactions and mechanisms, it would be important to explore other effectors of Rab39, as well as any potential GEFs or GAPs. For example, a specific class of tethering proteins known as Golgins help guide vesicles destined for the Golgi to the correct cisternae. These proteins have been shown to bind with Rab family G proteins (Sinka et al 2008). A few of these tethering proteins that would be interesting to study in relation to Rab39 would be GCC88, Golgin-245, Golgin-97, and Golgin-84. Although there are no strong candidates yet, investigating potential GEFs and GAPs of Rab39 would provide insight into its regulation.

Finally, further testing must be done to determine the role of Rab39 in acto-myosin organization. First, an actin marker must be observed in Rab39 shRNA embryos, and a myosin marker must be observed in Klp98A shRNA embryos to make sure that those results are consistent to the results provided here. Additionally, more experiments must be conducted in order to resolve whether acto-myosin organization in furrows is dependent specifically on the Rab39 pathway, or just on membrane addition in general. To accomplish this, another pathway involved in membrane addition, such as the RalA pathway (Holly et al 2018), must be disrupted and actin and myosin observed. If the results obtained in this experiment are similar then it is possible acto-myosin distribution is just dependent on successful membrane addition. Looking at upstream activators of myosin, such as Rho kinases, in Rab39 shRNA embryos would also help determine if the Rab39 pathway is involved with myosin activation.

REFERENCES

Albertson R, Riggs B, Sullivan W. Membrane traffic: a driving force in cytokinesis. *Trends Cell Biol*. 2005;15(2):92-101.

Altan-Bonnet N, Phair RD, Polishchuk RS, Weigert R, Lippincott-Schwartz J. A role for Arf1 in mitotic Golgi disassembly, chromosome segregation, and cytokinesis. *Proc Natl Acad Sci U S A*. 2003;100(23):13314-13319.

Baker J, Theurkauf WE, Schubiger G. Dynamic changes in microtubule configuration correlate with nuclear migration in the preblastoderm Drosophila embryo. *J Cell Biol*. 1993;122(1):113-121.

Chen, T., Han, Y., Yang, M., Zhang, W., Li, N., Wan, T., Cao, X. (2003). Rab39, a novel Golgi-associated Rab GTPase from human dendritic cells involved in cellular endocytosis. *Biochemical and Biophysical Research Communications*, *303*(4), 1114–1120.

Derivery E, Seum C, Daeden A, et al. Polarized endosome dynamics by spindle asymmetry during asymmetric cell division. *Nature*. 2015;528(7581):280-285.

Drechsel DN, Hyman AA, Hall A, Glotzer M. A requirement for Rho and Cdc42 during cytokinesis in Xenopus embryos. *Curr Biol*. 1997;7(1):12-23.

D'Souza Z, Blackburn JB, Kudlyk T, Pokrovskaya ID, Lupashin VV. Defects in COG-Mediated Golgi Trafficking Alter Endo-Lysosomal System in Human Cells. *Front Cell Dev Biol*. 2019;7:118.

Echard A, Jollivet F, Martinez O, et al. Interaction of a Golgi-associated kinesin-like protein with Rab6. *Science*. 1998;279(5350):580-585.

Farkas RM, Giansanti MG, Gatti M, Fuller MT. The Drosophila Cog5 homologue is required for cytokinesis, cell elongation, and assembly of specialized Golgi architecture during spermatogenesis. *Mol Biol Cell*. 2003;14(1):190-200.

Figard L, Xu H, Garcia HG, Golding I, Sokac AM. The plasma membrane flattens out to fuel cell-surface growth during Drosophila cellularization. *Dev Cell*. 2013;27(6):648-655.

Foe VE, Alberts BM. Studies of nuclear and cytoplasmic behaviour during the five mitotic cycles that precede gastrulation in Drosophila embryogenesis. *J Cell Sci*. 1983;61:31-70.

Fullilove SL, Jacobson AG. Nuclear elongation and cytokinesis in Drosophila montana. *Dev Biol*. 1971;26(4):560-577. doi:10.1016/0012-1606(71)90141-2
Gambarte Tudela J, Buonfigli J, Luján A, et al. Rab39a and Rab39b Display Different Intracellular Distribution and Function in Sphingolipids and Phospholipids Transport. *Int J Mol Sci*. 2019;20(7):1688.

Gillingham, A. K., Sinka, R., Torres, I. L., Lilley, K. S., & Munro, S. (2014). Toward a comprehensive map of the effectors of rab GTPases. *Developmental cell*, *31*(3), 358–373.

Grosshans BL, Ortiz D, Novick P. Rabs and their effectors: achieving specificity in membrane traffic. *Proc Natl Acad Sci U S A*. 2006;103(32):11821-11827.

He B, Martin A, Wieschaus E. Flow-dependent myosin recruitment during Drosophila cellularization requires zygotic dunk activity. *Development*. 2016;143(13):2417-2430.

Hill E, Clarke M, Barr FA. The Rab6-binding kinesin, Rab6-KIFL, is required for cytokinesis. *EMBO J*. 2000;19(21):5711-5719.

Holly, R. M., Mavor, L. M., Zuo, Z., & Blankenship, J. T. (2015). A rapid, membrane-dependent pathway directs furrow formation through RalA in the early Drosophila embryo. *Development (Cambridge, England)*, *142*(13), 2316–2328

Jewett, C. E., Vanderleest, T. E., Miao, H., Xie, Y., Madhu, R., Loerke, D., & Blankenship, J. T. (2017). Planar polarized Rab35 functions as an oscillatory ratchet during cell intercalation in the Drosophila epithelium. *Nature communications*, *8*(1), 476.

Li BJ, Chen H, Jiang SS, et al. PX Domain-Containing Kinesin KIF16B and Microtubule-Dependent Intracellular Movements. *J Membr Biol*. 2020;253(2):101-108.

Mauvezin C, Neisch AL, Ayala CI, et al. Coordination of autophagosome-lysosome fusion and transport by a Klp98A-Rab14 complex in Drosophila. *J Cell Sci*. 2016;129(5):971-982.

Mauvezin C, Neufeld TP. Autophagosomes take the Klp98-A train. *Small GTPases*. 2017;8(1):16-19.

Mavor LM, Miao H, Zuo Z, et al. Rab8 directs furrow ingression and membrane addition during epithelial formation in Drosophila melanogaster. *Development*. 2016;143(5):892-903.

Mitra S, Cheng KW, Mills GB. Rab GTPases implicated in inherited and acquired disorders. *Semin Cell Dev Biol*. 2011;22(1):57-68

Papoulas O, Hays TS, Sisson JC. The golgin Lava lamp mediates dynein-based Golgi movements during Drosophila cellularization. *Nat Cell Biol*. 2005;7(6):612-618.

Pfeffer SR. Structural clues to Rab GTPase functional diversity. *J Biol Chem*. 2005;280(16):15485-15488.

Recchi C, Seabra MC. Novel functions for Rab GTPases in multiple aspects of tumour progression. *Biochem Soc Trans*. 2012;40(6):1398-1403.

Ripoche J, Link B, Yucel JK, Tokuyasu K, Malhotra V. Location of Golgi membranes with reference to dividing nuclei in syncytial Drosophila embryos. *Proc Natl Acad Sci U S A*. 1994;91(5):1878-1882.

Sisson JC, Field C, Ventura R, Royou A, Sullivan W. Lava lamp, a novel peripheral golgi protein, is required for Drosophila melanogaster cellularization. *J Cell Biol*. 2000;151(4):905-918.

Sinka R, Gillingham AK, Kondylis V, Munro S. Golgi coiled-coil proteins contain multiple binding sites for Rab family G proteins. *J Cell Biol*. 2008;183(4):607-615.

Xie, Y., & Blankenship, J. T. (2018). Differentially-dimensioned furrow formation by zygotic gene expression and the MBT. *PLoS genetics*, *14*(1), e1007174

Zhang J, Schulze KL, Hiesinger PR, et al. Thirty-one flavors of Drosophila rab proteins. *Genetics*. 2007;176(2):1307-1322.